Asian Journal of Chemistry; Vol. 24, No. 10 (2012), 4709-4712

ASIAN JOURNAL OF CHEMISTRY

www.asianjournalofchemistry.co.in

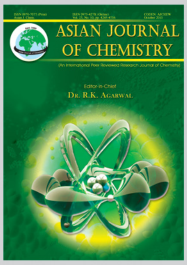

Preparation and Characterization of N, S Co-doped TiO_2 Nanopowder and its Photocatalytic Activity under Visible Light

S.Z. Hu*, F.Y. Li and Z.P. Fan

Institute of Eco-environmental Sciences, Liaoning Shihua University, Fushun 113001, P.R. China

*Corresponding author: Tel: +86 24 23847473; E-mail: hushaozheng001@163.com

(*Received*: 29 August 2011; *Accepted*: 12 May 2012) AJC-11474

N, S co-doped TiO_2 was prepared *via* a hydrothermal process. X-ray diffraction, UV-VIS spectroscopy and X-ray photoelectron spectroscopy were conducted to characterize the prepared TiO_2 particles. The results indicated that N and S doped into the TiO_2 crystal lattice simultaneously by hydrothermal process. The photocatalytic performance in the degradation of methylene blue indicated that N and S doped TiO_2 showed much higher photocatalytic activity than pure TiO_2 under visible light. Co-doping sample exhibited the highest activity. This is probably due to the synergistic effect of reduced particle size, optimal anatase/rutile ratio, reduced electron-hole recombination rate and more absorption in visible light region.

Key Words: TiO_2, Photocatalysis, Visible light, Co-doping, Hydrothermal method.

INTRODUCTION

Titania is the most widely used photocatalyst in photodegradation of organic pollutants in air and water[1,2]. However, TiO_2 can be activated only under UV-light irradiation due to its large band gap value of 3.2 eV. Therefore, it is indispensable to develop a TiO_2 photocatalyst with a high level of activity under visible light. In the past, transition metal cations have been used as dopants to red shift the absorption edge of TiO_2 to a visible-light region. However, the disadvantage of metal cation dopants is that they can serve as recombination centers for photogenerated electron-hole pairs, leading to a decreased activity[3]. Recently, anion (C, N, S, F, B) doped TiO_2 photocatalysts that show a relatively high level of activity under visible-light irradiation have been reported[4-8]. These non-metal elements have been proved to be beneficial doping elements in the TiO_2 through mixing their p orbital with O 2p orbital to reduce the band gap energy of TiO_2.

In order to further improve the photocatalytic activity, co-doped titania with double non-metal elements has attracted more attention. Li *et al.*[9] prepared N-F-codoped TiO_2 powders by spray pyrolysis and the prepared catalyst showed the high visible-light activity for decompositions of both acetaldehyde and trichloroethylene. They demonstrated that the high activity was ascribed to a synergetic consequence of several beneficial effects induced by the N-F codoping. Liu and Gao[10] synthesized (S, N)-codoped TiO_2 photocatalyst using a hydrothermal method and subsequent nitridation under NH_3 flow at 873 K for 4 h. Yu *et al.*[11] developed N, S-codoped TiO_2 by hydrolysis of $Ti(SO_4)_2$ in a $NH_3{\cdot}H_2O$ solution. They demonstrated that the photocatalytic activity of the as-prepared TiO_2 powders calcined at a temperature range of 400-700 ºC are obviously higher than that of P25.

Hydrothermal synthesis is one of the effective approaches to synthesizing nano-sized metal oxides[12,13]. It is a very simple method and does not require any special equipment. It provides a facile route to control particle size, particle morphology, microstructures, phase composition and surface chemical properties by means of adjusting synthesis conditions such as temperature, time and pH value of solution. Moreover, hydrothermal reaction takes place at a relatively low reaction temperature and no post-calcination generally is needed in the synthesis of crystalline metal oxide particles.

In the present work, a single anatase phase of N, S codoped TiO_2 photocatalyst had been prepared by a one-step low-temperature hydrothermal method using cheaper material $TiCl_4$ as Ti source, urea and thiourea as N and S sources. The prepared co-doped TiO_2 catalysts were tested in the photocatalytic degradation of methylene blue under visible light. A possible mechanism for the photocatalysis was also proposed.

EXPERIMENTAL

The N, S-codoped TiO_2 was synthesized by hydrothermal method. 0.8 mL of $TiCl_4$ was added dropwise into 20 mL de-ionized water at 0 ºC under stirring to obtain solution A. 0.3 g thiourea and 0.2 g urea were dissolved in 10 mL deionized water at room temperature to form solution B. The above solutions were mixed and stirred for 10 min. The resulting mixture was transferred into a 30 mL stainless steel autoclave and heated at 120 ºC for 12 h. The yellow precipitate was washed with deionized water, separated by centrifugation and dried at room temperature overnight under vacuum. The obtained TiO_2 powders were denoted as NS-TO. For comparison, N-TO and S-TO were prepared by the same procedure but in the absence of thiourea and presence of thiourea, respectively. Un-doped TiO_2 (TO) was prepared by the same precedure but in the absence of thiourea and thiourea, simultaneously.

XRD patterns of the prepared TiO_2 samples were recorded on a Rigaku D/max-2400 instrument using CuK_α radiation (λ = 1.54 Å). UV-VIS spectroscopy measurement was carried out on a JASCO V-550 model UV-VIS spectrophotometer, using $BaSO_4$ as the reflectance sample. XPS measurements were conducted on a Thermo Escalab 250 XPS system with Al Ka radiation as the exciting source. The binding energies were calibrated by referencing the C 1s peak (284.6 eV) to reduce the sample charge effect.

Methylene blue was selected as model compound to evaluate the photocatalytic performance of the prepared TiO_2 particles in an aqueous solution under visible light irradiation. 0.1 g TiO_2 powders were dispersed in 100 mL aqueous solution of methylene blue (50 ppm) in an ultrasound generator for 10 min. The suspension was transferred into a self-designed glass reactor and stirred for 0.5 h in darkness to achieve the adsorption equilibrium. In the photoreaction under visible light irradiation, the suspension was exposed to a 110-W high-pressure sodium lamp with main emission in the range of 400-800 nm and air was bubbled at 130 mL/min through the solution. The UV light portion of sodium lamp was filtered by 0.5 M $NaNO_2$ solution. All runs were conducted at ambient pressure at 30 ºC. At given time intervals, 4 mL suspension was taken and immediately centrifuged to separate the liquid samples from the solid catalyst. The concentrations of methylene blue before and after reaction were measured by means of a UV-VIS spectrophotometer at a wavelength of 665 nm. The percentage of degradation D % was determined as follows:

$$D\% = \frac{A_0 - A}{A_0} \times 100\% \qquad (1)$$

where, A_0 and A are the absorbances of the liquid sample before and after degradation, respectively.

RESULTS AND DISCUSSION

The XRD patterns of the prepared catalysts (Fig. 1) indicated that all TiO_2 samples were mixture of anatase and rutile phases. The particle sizes of the catalysts were calculated by their XRD patterns according to the Debye-Scherrer equation[14]. The results indicated that anatase/rutile ratio is almost 1:1 for titanium dioxide (TO). After S doping, the obtained S-TO and NS-TO exhibited a higher anatase/rutile ratio (3:1) compared with TO. This indicated that S doping imprved the formation of anatase TiO_2. The particle size of TO was around 20 nm. After N doping, the prepared N-TO and NS-TO showed a much smaller particle sizes (13 nm). Therefore, it is deduced that N doping could restrain the particle growth during the hydrothermal process.

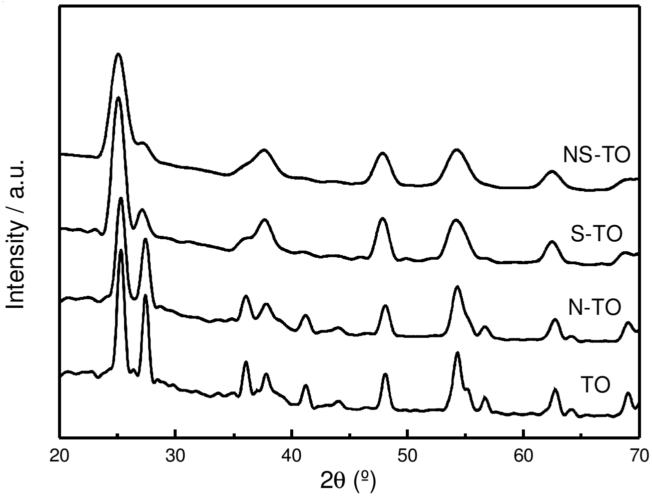

Fig. 1. XRD patterns of the prepared catalysts

The UV-VIS diffuse reflectance spectra of prepared catalysts are shown in Fig. 2. Undoped TO showed no absorption in the visible light region. However, after doping, N-TO, S-TO and NS-TO exhibited obvious absorption into the visible light region. The co-doped sample NS-TO exhibited the strongest visible light absorption. These absorption in the visible light region is possibly due to the incorporation of nitrogen or sulfur into TiO_2 framework, leading to a slight alteration of crystal and electronic structures. TiO_2 is an indirect gap semiconductor. The band gap can be estimated from the tangent lines in the plots of the square root of the Kubelka-Munk functions against the photon energy[15]. The calculated band gap energies of prepared samples were all 3.0 eV. According to the report of Irie *et al.*[16], the doping did not narrow the band gap but formation a isolated narrow band located above the valence band which is responsible for this visible light response.

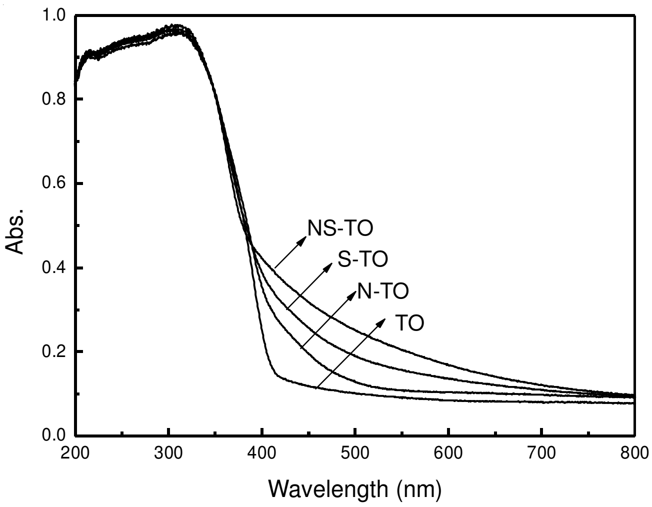

Fig. 2. UV-VIS diffuse reflectance spectra of prepared catalysts

Fig. 3 shows the X-ray photoelectron (XPS) spectra of prepared samples in the region of S 2p (a), N 1s (b) and Ti 2p (c). In the spectrum of S 2p region (Fig. 3a), the peak around 168.2 eV which attributed to S^{6+} was observed for NS-TO. This indicated that the sulfur atoms (S^{6+}) substituted Ti^{4+} to incorporate into TiO_2 framework.

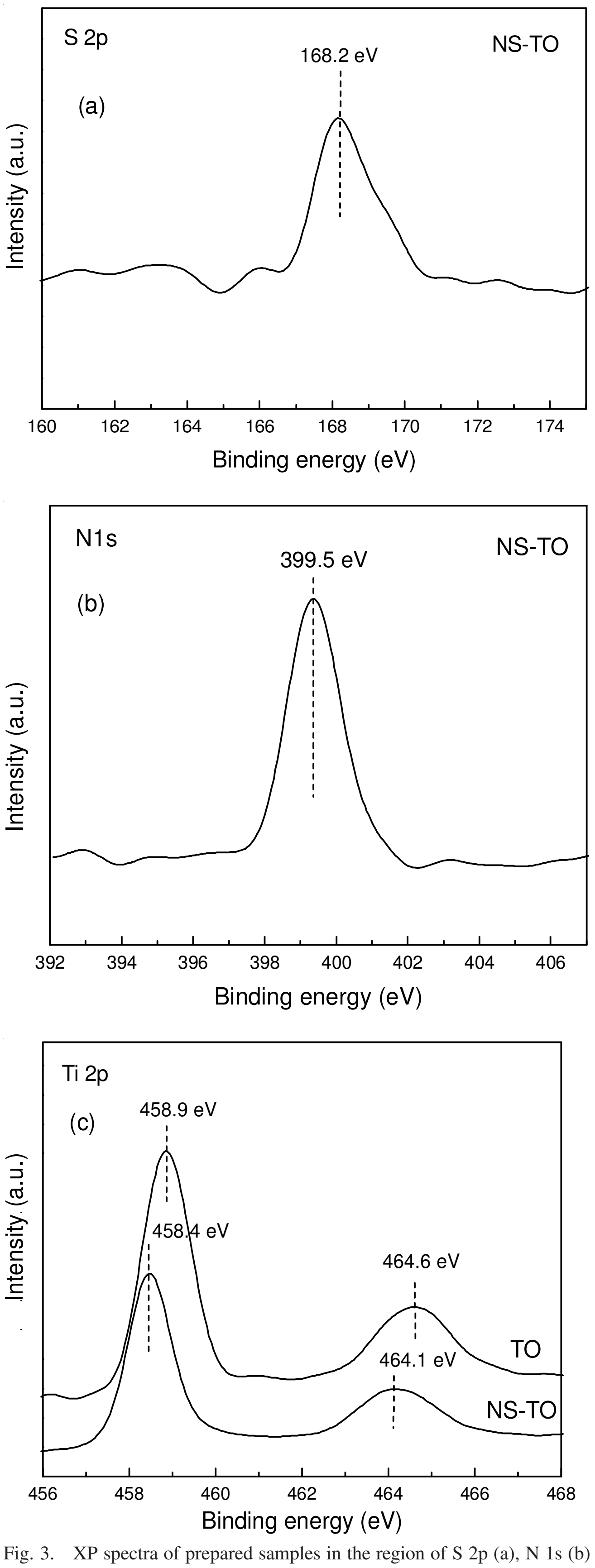

Fig. 3. XP spectra of prepared samples in the region of S 2p (a), N 1s (b) and Ti 2p (c)

Up to now, the assignment of the XPS peak of N 1s is still under debate. Since the preparation methods and conditions considerably affect nitrogen XPS spectral features, the peak positions may be different from different literatures. In addition, the different nitrogen source may also influence the characteristics of the nitrogen state. Cong *et al.*[17] reported that the peak in the range of 397-401 eV was the N 1s peak when using the wet chemical method. In the region of N 1s (Fig. 3b), the N 1s peak of NS-TO is around 399.5 eV, which is attributed to the N 1s electron binding energy of the N atom in the environment of O-Ti-N[18]. This binding energy is higher than the typical binding energy of 396.9 eV in TiN. When nitrogen replaces the oxygen in the O-Ti-O structure, the electron density around N will be reduced. Thus, the N1s binding energy in an O-Ti-N environment is higher than that in an N-Ti-N environment. In the region of Ti 2p (Fig. 3c), an obvious shift to lower binding energy was observed for NS-TO compared with undoped TO. The shifts of binding energy for Ti^{4+} species may be associated with the formation of S-Ti-O and N-Ti-O structure in NS-TO after doping. Due to the higher electronegativity of oxygen, partial electrons of S and N might be transferred to Ti, leading to the increased electron density of Ti. This increased electron density led to the decreased binding energy of NS-TO.

Photoluminescence emission spectra are used to determine the efficiency of trapping, migration and transfer of a charge carrier and to understand the fate of electron-hole pairs in semiconductors[19]. Fig. 4 shows the photoluminescence spectra of the prepared catalysts using excitation at 241 nm. The photoluminescence intensity of TiO_2 was stronger than the photoluminescence intensities of doping samples. This phenomenon may result from the photoluminescence quenching after N and S doping in TiO_2. Most of the electrons and holes recombine within a few nanoseconds in the absence of scavengers. If scavengers or surface defects are present to trap the electrons or holes, the electron-hole recombination can be suppressed, leading to an enhancement of the subsequent photocatalytic reactions[20]. It is shown that NS-TO shows the lowest photoluminescence intensity, indicating the electron-hole recombination restrained effectively after N, S codoping.

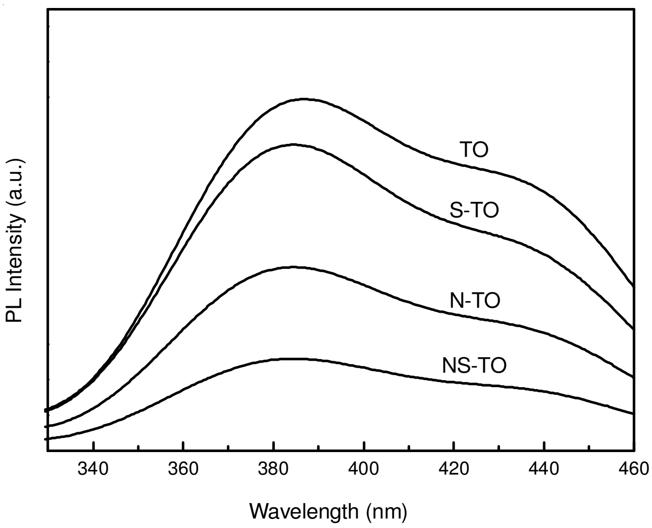

Fig. 4. Photoluminescence emission spectra of prepared catalysts

The photocatalytic activities of prepared samples under visible light are shown in Fig. 5. Titanium dioxide (TO) has no photocatalytic activity for the degradation of methylene blue, whereas *N*-TO, S-TO and NS-TO exhibited much higher photocatalytic activities than TO. This may be attributed to the reduced particle size, optimal anatase/rutile ratio and enhanced visible light absorption. The number of surface active sites will increase with reducing the particle size, leading to the increase in the surface charge carrier transfer rate in photocatalysis process and thus to the decrease in the electron-hole recombination[1,2]. It is generally accepted that TiO_2 with an anatase/rutile ratio of 3, such as NS-TO, showed the highest photocatalytic activity[21]. The interface between the two phases may act as a rapid separation site for the photo-generated electrons and holes due to the difference in the energy level of their conduction bands and valence bands. NS-TO showed the highest photocatalytic activity among the samples. Besides the reduced particle size, optimal anatase/rutile ratio and reduced electron-hole recombination rate, another important reason is probably due to NS-TO absorbed more visible light, leading to its better visible light utilization rate than other samples.

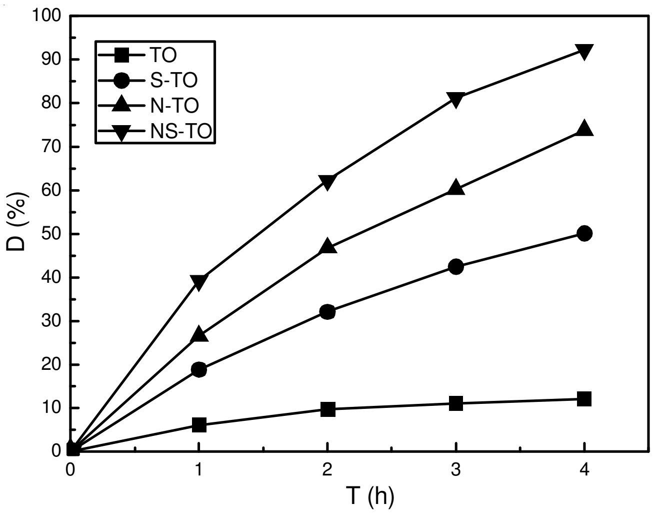

Fig. 5. Photocatalytic activities of prepared catalysts under visible light

Conclusion

N, S co-doped TiO_2 was prepared by a hydrothermal process. The particle size of prepared sample was reduced by N doping. The S doping imprved the formation of anatase TiO_2. The N, S co-doped TiO_2 absorbed more visible light than other samples. TO has no photocatalytic activity for the degradation of methylene blue, whereas N-TO, S-TO and NS-TO exhibited much higher photocatalytic activities. NS-TO exhibited the highest activity, probably due to the synergistic effect of reduced particle size, optimal anatase/rutile ratio, reduced electron-hole recombination rate and more absorption in visible light region.

ACKNOWLEDGEMENTS

This work was supported by National Natural Science Foundation of China (No. 41071317, 30972418), National Key Technology R & D Programme of China (No. 2007BAC16B07) and the Natural Science Foundation of Liaoning Province (No. 20092080).

REFERENCES

1. M.R. Hoffmann, S.T. Martin, W. Choi and D.W. Bahnemann, *Chem. Rev.*, **95**, 69 (1995).
2. A. Fujishima, T.N. Rao and D.A. Tryk, *J. Photochem. Photobiol. C*, **1**, 1 (2000).
3. W. Choi, A. Termin and M.R. Hoffmann, *J. Phys. Chem.*, **98**, 13669 (1994).
4. Y.N. Huo, Z.F. Bian, X.Y. Zhang, Y. Jin, J. Zhu and H.X. Li, *J. Phys. Chem. C*, **112**, 6546 (2008).
5. H.J. Sun, H.L. Liu, J. Ma, X.Y. Wang, B. Wang and L. Han, *J. Hazard. Mater.*, **156**, 552 (2008).
6. A. Zaleska, J.W. Sobczak, E. Grabowska and J. Hupka, *Appl. Catal. B*, **78**, 92 (2008).
7. W.J. Ren, Z.H. Ai, F.L. Jia, L.Z. Zhang, X.X. Fan and Z.G. Zou, *Appl. Catal. B*, **69**, 138 (2007).
8. G.S. Wu and A.C. Chen, *J. Photochem. Photobiol. A.*, **195**, 47 (2008).
9. D. Li, N. Ohashi, S. Hishita, T. Kolodiazhnyi and H. Haneda, *J. Solid State Chem.*, **178**, 3293 (2005).
10. H.Y. Liu and L. Gao, *J. Am. Ceram. Soc.*, **87**, 1582 (2004).
11. J.G. Yu, M.H. Zhou, B. Cheng and X.J. Zhao, *J. Mol. Catal. A.*, **246**, 176 (2006).
12. H.M. Cheng, J.M. Ma, Z.G. Zhao and L.M. Qi, *Chem. Mater.*, **7**, 663 (1995).
13. C.C. Wang and J.Y. Ying, *Chem. Mater.*, **11**, 3113 (1999).
14. J. Lin, Y. Lin, P. Liu, M.J. Meziani, L.F. Allard and Y.P. Sun, *J. Am. Chem. Soc.*, **124**, 11514 (2002).
15. Y.I. Kim, S.J. Atherton, E.S. Brigham and T.E. Mallouk, *J. Phys. Chem.*, **97**, 11802 (1993).
16. H. Irie, Y. Watanaba and K. Hashimoto, *J. Phys. Chem. B*, **107**, 5483 (2003).
17. Y. Cong, J.L. Zhang, F. Chen, M. Anpo and D.N. He, *J. Phys. Chem. C*, **111**, 10618 (2007).
18. X.C. Wang, J.C. Yu, Y.L. Chen, L. Wu and X.Z. Fu, *Environ. Sci. Technol.*, **40**, 2369 (2006).
19. Y. Cong, J. Zhang, F. Chen and M. Anpo, *J. Phys. Chem. C*, **111**, 6976 (2007).
20. W.J. Fa, L. Zan, C.Q. Gong, J.C. Zhong and K.J. Deng, *Appl. Catal. B*, **79**, 216 (2008).
21. Z. Ding, G.Q. Lu and P.F. Greenfield, *J. Phys. Chem. B*, **104**, 4815 (2004).